

UCLA

UCLA Previously Published Works

Title

Differentiation Capacity of Human Mesenchymal Stem Cells into Keratocyte Lineage

Permalink

<https://escholarship.org/uc/item/67j764p3>

Journal

Investigative Ophthalmology & Visual Science, 60(8)

ISSN

0146-0404

Authors

Dos Santos, Aurelie
Balayan, Alis
Funderburgh, Martha L
[et al.](#)

Publication Date

2019-07-16

DOI

10.1167/iovs.19-27008

Peer reviewed

Differentiation Capacity of Human Mesenchymal Stem Cells into Keratocyte Lineage

Aurelie Dos Santos,¹ Alis Balayan,¹ Martha L. Funderburgh,² John Ngo,¹ James L. Funderburgh,² and Sophie X. Deng¹

¹Stein Eye Institute, University of California Los Angeles, Los Angeles, California, United States

²Eye and Ear Institute, University of Pittsburgh, Pittsburgh, Pennsylvania, United States

Correspondence: Sophie X. Deng, Stein Eye Institute, University of California Los Angeles, 100 Stein Plaza, Los Angeles, CA, USA; deng@jsei.ucla.edu.

James L. Funderburgh, UPMC Eye Center, Eye and Ear Institute, Ophthalmology and Visual Science Research Center, Department of Ophthalmology, University of Pittsburgh School of Medicine, 203 Lothrop Street, Pittsburgh, PA 15213, USA; jlfunder@pitt.edu

Submitted: March 4, 2019

Accepted: June 13, 2019

Citation: Dos Santos A, Balayan A, Funderburgh ML, Ngo J, Funderburgh JL, Deng SX. Differentiation capacity of human mesenchymal stem cells into keratocyte lineage. *Invest Ophthalmol Vis Sci.* 2019;60:3013-3023. <https://doi.org/10.1167/iovs.19-27008>

PURPOSE. Mesenchymal stem cells (MSCs) have been extensively studied for their capacity to enhance wound healing and represent a promising research field for generating cell therapies for corneal scars. In the present study, we investigated MSCs from different tissues and their potential to differentiate toward corneal keratocytes.

METHODS. Adipose-derived stem cells, bone marrow MSCs, umbilical cord stem cells, and corneal stromal stem cells (CSSCs) were characterized by their expression of surface markers CD105, CD90, and CD73, and their multilineage differentiation capacity into adipocytes, osteoblasts, and chondrocytes. MSCs were also evaluated for their potential to differentiate toward keratocytes, and for upregulation of the anti-inflammatory protein TNF α -stimulated gene-6 (TNFAIP6) after simulation by IFN- γ and TNF- α .

RESULTS. Keratocyte lineage induction was achieved in all MSCs as indicated by the upregulated expression of keratocyte markers, including keratocan, lumican, and carbohydrate sulfotransferase. TNFAIP6 response to inflammatory stimulation was observed only in CSSCs; increasing by 3-fold compared with the control ($P < 0.05$).

CONCLUSIONS. Based on our findings, CSSCs appeared to have the greatest differentiation potential toward the keratocyte lineage and the greatest anti-inflammatory properties in vitro.

Keywords: mesenchymal stem cells, keratocyte, corneal repair

Corneal diseases are one of the leading causes of blindness, affecting millions of individuals worldwide.^{1,2} The routine treatment for corneal blindness is corneal transplantation or keratoplasty. Despite the high number of transplantations, keratoplasty is invasive and associated with intraoperative and postoperative complications, including bleeding, immune rejection, wound dehiscence, and infection.³ In addition, there is a severe shortage of corneal tissues.⁴ As a result, there is a pressing need to develop alternative treatments for corneal blindness. Alternative treatments for corneal opacity that are currently being explored include keratoprosthesis,⁵ bioengineered corneal tissue,⁶ and cell-based therapy.^{7,8} Recent studies have shown that cell-based therapy using mesenchymal stem cells (MSCs) may be effective for corneal stromal repair that avoids corneal transplantation.^{9,10}

MSCs are multipotent, self-renewing adult stem cells. They are characterized by the expression of stem cell/progenitor cell markers and are able to differentiate into cells of various lineages. MSCs have been isolated from diverse tissues such as bone marrow,¹¹ adipose,¹² umbilical cord,¹³ and dental tissues,¹⁴ as well as from the corneal stroma.¹⁵ MSCs are of particular interest in recent years because they exhibit regenerative potential and anti-inflammatory properties through their paracrine activity.¹⁶ MSCs can migrate to the site of injury and secrete anti-inflammatory factors to suppress inflammation and promote wound healing.¹⁷ As such, TNF- α -stimulated gene-6 (TSG-6), an anti-inflammatory protein, was

found to have an important role in the reduction of inflammation and scarring of corneal wounds.^{8,18} The mechanisms by which TSG-6 mediates its effects is through the reduction of neutrophil migration to the corneal wound. TSG-6 was also described as a biomarker for human MSCs in vivo: the expression of TSG-6 was predictive of the inflammation-modulating effect when the cells were applied in a model of corneal injury.¹⁹ Production of TSG-6 by MSCs posits a parameter to identify the MSC type with the greatest anti-inflammatory and scar-minimizing properties.

Previous studies demonstrated that MSCs have the plasticity to differentiate into keratocytes, corneal stromal cells in vivo²⁰⁻²² and in vitro.^{21,23-29} Keratocytes are mesenchymal-derived cells³⁰ that contribute to the homeostasis and transparency^{31,32} of the cornea with the expression of crystalline proteins, such as aldehyde dehydrogenase 3A1,³³ proteoglycans, such as lumican and keratocan, as well as a carbohydrate sulfotransferase required for keratan sulfate biosynthesis.²⁶ In the healthy cornea, keratocytes are quiescent cells.³⁴ Upon corneal injury, keratocytes reenter the cell cycle³¹ and play an important role in the wound-healing progression of corneal tissue by either undergoing cell death or transitioning to a corneal fibroblast or myofibroblast phenotype.³¹ Corneal fibroblasts secrete metalloproteinases that may be involved in extracellular matrix remodeling,³⁵ whereas myofibroblasts contribute to the wound closure and production of fibrotic extracellular matrix in the injured cornea.³⁵ The wound-healing

process by default leads to corneal stromal fibrosis and scar formation resulting in corneal opacity.³⁶ Understanding the capacity of MSCs to differentiate into corneal keratocytes could provide additional information about the potential of MSCs in cell therapy for corneal repair.

In this study, we investigate four different types of MSCs: adipose-derived stem cells (ASCs), bone marrow MSCs (BMMSCs), umbilical cord stem cells (UCSCs), and corneal stromal stem cells (CSSCs). The aim of this study was to provide insights about the plasticity of MSCs toward corneal keratocyte lineage, their anti-inflammatory properties, and their putative application for corneal stromal repair.

MATERIALS AND METHODS

Cell Culture

Experimentation on human tissue adhered to the tenets of the Declaration of Helsinki. The experimental protocol was evaluated and exempted by the University of California, Los Angeles Institutional Review Boards. Consent was obtained for the tissues to be used for research. CSSCs were isolated and propagated as previously described.³⁷ BMMSCs from two donors (STEMCELL Technologies, Inc., Vancouver, Canada) were used in this study. UCSCs were isolated from umbilical cords from two donors and were propagated according to the method of Reinisch and Strunk.³⁸ ASCs from a single donor at passage 1 were a gift from J. Peter Rubin's laboratory (University of Pittsburgh Medical Center).

CSSCs were cultured on fibronectin-coated cell culture plasticware (FNC coating solution; AthenaES, Baltimore, MD, USA), with MCDB201/Dulbecco's modified Eagle's medium (DMEM) low glucose-based medium supplemented with 2% human serum (Innovative Research, Inc., Perary Court Novi, MI, USA) as previously described.³⁸ ASCs, BMMSCs, and UCSCs were maintained in culture in minimum essential medium- α supplemented with 10% fetal bovine serum and penicillin/streptomycin (Gibco, Waltham, MA, USA). Cells were passaged (TrypLE, Life Technologies, Carlsbad, CA, USA) when 80% to 90% confluence was reached. Cells from passages 2 to 5 were used in the study.

Flow Cytometry

MSCs were characterized by the expression of the MSC-specific surface antigens CD105, CD90, and CD73 (>90% of the cells expressed each marker) and the low or absent expression of hematopoietic markers CD14, CD20, CD34, and CD45 (<10% for of the cells expressed each marker); a phenotyping kit (Miltenyi Biotec, Bergisch Gladbach, Germany) was used for analysis of antigen expression. The analysis was performed with a FACSAria flow cytometer (BD Bioscience, San Jose, CA, USA) at the flow cytometry core facility at the Eye and Ear Institute of Pittsburgh. Fluorescence compensation settings were adjusted according to the kit's instructions. The LIVE/DEAD Fixable Aqua Dead Cell Stain Kit (Life Technologies, Carlsbad, CA, USA) was used to exclude dead cells. Data were analyzed by using FlowJo, LLC (v10.0.7; Ashland, OR, USA).

Multilineage Differentiation

Multilineage induction toward adipogenic, osteogenic, and chondrogenic fates was performed by using the MesenCult stimulatory and differentiation kits (Human; STEMCELL Technologies, Inc.). MSCs were plated at a cell density of $10^4/\text{cm}^2$ for adipogenic and osteogenic induction. When cells reached 70% to 80% confluence in culture, osteogenic differentiation was started by using the MesenCult Osteogenic Stimulatory Kit

(Human; STEMCELL Technologies, Inc.). Once multilayering of the cells was observed in culture, β -glycerophosphate (3.5 mM) was added to the stimulatory medium; the day of this occurrence was defined as day 0 of differentiation. The medium was changed every 3 days. At days 7 and 21 of differentiation, RNA was collected for gene expression analysis. MSC-derived osteoblasts were fixed at day 21 of differentiation by using 2.5% glutaraldehyde solution for 20 minutes at room temperature (RT), washing twice with PBS, and staining with Alizarin red solution for 20 minutes (EMD Millipore, Burlington, MA, USA). Adipogenic differentiation began when cells reached 100% confluence. The medium was changed to MesenCult Adipogenic Differentiation Medium (Human; STEMCELL Technologies, Inc.); the day of this occurrence marked day 0 of differentiation. The differentiation medium was renewed every 3 days. Cells were collected for RNA analysis at days 7 and 21 of differentiation.

Chondrogenic differentiation was assessed in the form of a 3-dimensional (3-D) pellet culture system (5×10^5 cells per pellet) as recommended by the manufacturer, using MesenCult-ACF Chondrogenic Differentiation Medium (STEMCELL Technologies, Inc.). Chondrogenic pellets were collected on day 7 of differentiation for transcript analysis. On day 21, chondrogenic pellets were fixed with 0.1% glutaraldehyde for 20 minutes at RT, then washed twice with PBS. Pellets were embedded in Tissue-Tek O.C.T. Compound (Sakura Finetek USA Inc., Torrance, CA, USA), cut into 7- μm sections, and stained with Alcian blue solution for 1 hour at RT (Sigma-Aldrich, Saint Louis, MO, USA).

Keratocyte differentiation was induced as follows. Briefly, MSCs were plated at a cell density of $10^4/\text{cm}^2$. When cells reached confluence, the medium was substituted with keratocyte differentiation medium that consisted of advanced DMEM (Gibco), antibiotics (penicillin, streptomycin, gentamicin), and L-ascorbic acid 2-phosphate (1 mM; Sigma-Aldrich), and was supplemented with recombinant human TGF- β 3 (1 ng/mL; R&D Systems, Minneapolis, MN, USA) and recombinant human FGF2 (10 ng/mL; Abcam, Cambridge, UK). The differentiation medium was changed every 3 days, and samples were collected for RNA analysis at day 7 of differentiation.

TNFAIP6 Expression

MSCs were plated at a cell density of $10^4/\text{cm}^2$. The next day, cells were treated with recombinant human TNF- α (10 ng/mL; PeproTech, Rocky Hill, NJ, USA) and recombinant human INF- γ (25 ng/mL; PeproTech) for 16 hours. Samples were then collected for gene expression analysis of TSG-6 transcript.

RNA Extraction, cDNA Transcription, and Real-Time PCR

RNA was isolated by using a RNA Mini isolation kit (Qiagen Inc., Germantown, MD, USA). After RNA elution from the column, RNA was precipitated overnight with 450 mM ammonium acetate (Life Technologies), 200 ng/mL GlycoBlue coprecipitant (Life Technologies), and 100% ethanol (Sigma-Aldrich). RNA concentration was measured by the NanoDrop 2000 spectrophotometer (v. 1.6.198; ThermoFisher, Waltham, MA, USA), and 1 μg of RNA was used per transcription reaction using Superscript III Reverse Transcriptase (100 U/ μg of RNA; Life Technologies). Primers for real-time PCR (RT-PCR) are listed in Supplementary Table S1. RT-PCR was performed with SYBR Green Master Mix (Applied Biosystems, Carlsbad, CA, USA) in an Eppendorf Mastercycler ep realplex (v2.2; Eppendorf, Hauppauge, NY, USA). Two housekeeping genes were used per sample for normalization of the data. Crossing

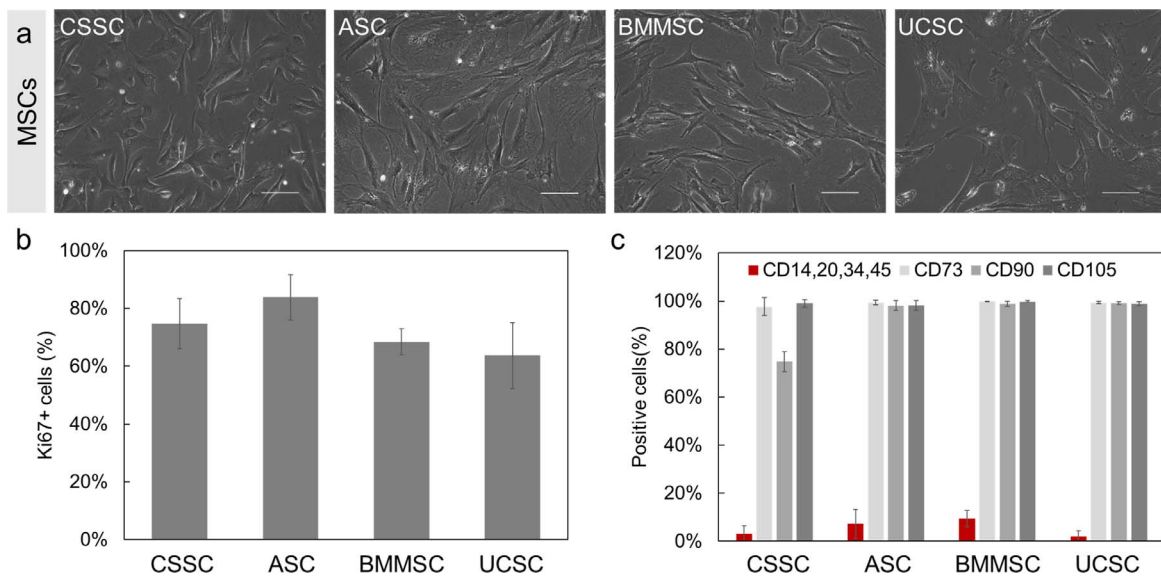


FIGURE 1. Morphology and characterization of the different MSCs investigated. (a) Phase-contrast images of MSCs: CSSC, ASC, BMMSC, and UCSC. Scale bar: 100 μ m. (b) Proliferation of the MSCs: Ki67 proliferation marker was quantified by computing the percentage of number of Ki67-positive cells per number of 4',6-diamidino-2-phenylindole positive cells using immunofluorescence staining. (c) Phenotyping of the MSCs was carried out by flow cytometry analysis of surface antigens CD73, CD90, CD105 (positive surface markers) and CD34, CD14, CD20, CD45 (negative surface markers, in red). Results are expressed as mean \pm SD ($n = 3$ independent experiments). $N = 2$ cell lines for BMMSCs and UCSCs.

threshold (Ct) values were obtained, and the relative expression level was calculated by the $2^{(-\Delta\Delta Ct)}$ formula using the expression in undifferentiated MSCs as the control.³⁹

Immunofluorescence

Cells were fixed with 4% paraformaldehyde (Electron Microscopy Sciences, Hatfield, PA, USA) in PBS for 15 minutes at 4°C and washed with PBS. Cells were permeabilized with 0.2% Triton (Sigma-Aldrich), and nonspecific antigens were blocked with 1% normal donkey serum (NDS) in PBS at RT for 30 minutes. Primary antibody incubation was performed overnight at 4°C in a solution that consisted of 0.2% Triton and 0.5% NDS. Antibodies used were specific to Ki67 (mouse; clone MIB-1; dilution ratio, 1:100; DAKO Omnis, Glostrup, Denmark), adiponectin (mouse; dilution ratio, 1:400; Abcam, Cambridge, UK), and BMI1 F6 (mouse; dilution ratio, 1:100; EMD Millipore). Donkey anti-mouse immunoglobulin conjugated to Alexa-Fluor 488 (dilution ratio, 1:400; Life Technologies) was used as the secondary antibody. Hoechst 33342 (Thermo-Fisher) was used for nuclear staining. Samples were mounted and analyzed.

Imaging

Imaging was performed with the fluorescence microscope BZ-X710 from Keyence Corporation (BZ-X Viewer version 01.03.00.05; Osaka, Japan). Pictures were taken with $\times 4$, $\times 10$, and $\times 20$ objectives.

Statistical Analysis

Statistical analysis was performed by using JMP Pro software (version 14.0.0). For two-pair comparisons, ANOVA followed by Student's *t*-test was performed. For multiple comparisons, ANOVA followed by Tukey's post hoc comparison of the means test was assessed.

RESULTS

Characterization of MSCs

All MSCs that we investigated exhibited a spindle-shaped morphology with a small cell body and short processes (Fig. 1a). The quantitation of the proliferation marker Ki67 indicated that more than 75% of the cell population of each MSC type were actively proliferating in early passages (passages 2 to 5) (Fig. 1b). The criteria used to identify MSCs as established by the International Society for Cellular Therapy (ISCT) are the expression of surface antigens CD105, CD73, and CD90 and the lack of expression of CD14, CD20, CD34, and CD45.⁴⁰ Using flow cytometry, we observed that more than 95% of the MSC populations expressed the surface antigens CD105 and CD73 (Fig. 1c). The surface antigen marker CD90 was present in more than 95% of the ASCs, BMMSCs, and UCSCs; only 75% of CSSCs expressed CD90. Fewer than 10% of the MSC populations expressed the negative surface markers CD14, CD20, CD34, and CD45.

The expression of B lymphoma Mo-MLV insertion region 1 homolog (BMI1) in MSCs was investigated. This protein is associated with maintenance of self-renewal and proliferation of stem cells and progenitor cells.⁴¹ BMI1, at the protein level, was detected by immunofluorescence staining in all of the MSC types (Fig. 2a).

As described previously, CSSCs express adult and pluripotent stem cell-associated genes such as ATP-binding cassette subfamily G member 2 (*ABCG2*), *NANOG*, and sex-determining region Ybox 2 (*SOX2*).^{15,37,42} Because these markers serve important roles such as chemoprotection (*ABCG2*) and maintenance of pluripotency (*SOX2* and *NANOG*), their expression was investigated in ASCs, BMMSCs, and UCSCs (Figs. 2b–d).⁴³ *ABCG2* expression was observed in all types of MSCs. CSSCs had the highest level of *ABCG2* expression ($P < 0.05$). The *ABCG2* transcript level was 4-fold lower in ASCs and BMMSCs and 2-fold lower in UCSCs than in CSSCs. For *NANOG* transcripts, expression in UCSCs was 4.6-fold higher than in CSSCs and 2-fold higher than in ASCs and BMMSCs ($P < 0.05$ for each

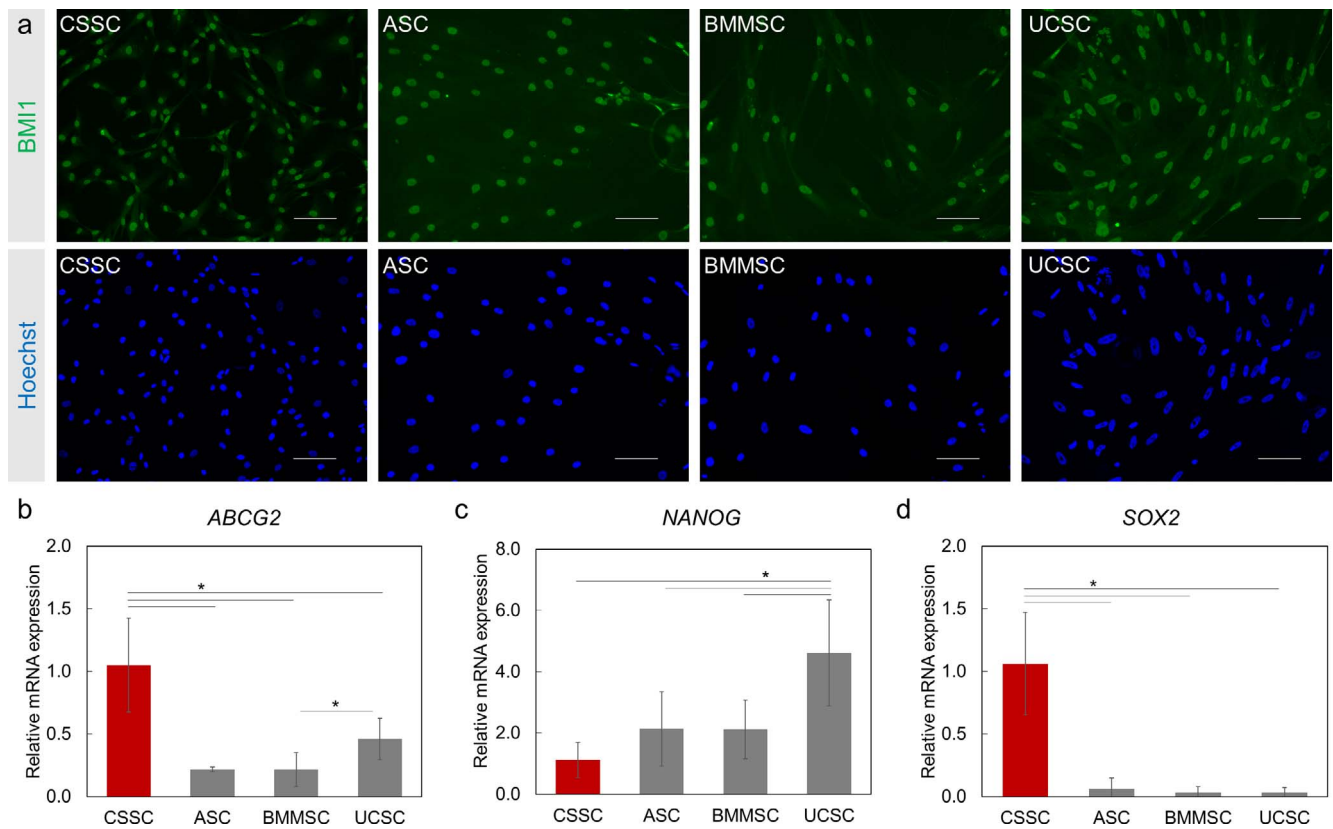


FIGURE 2. Expression of stem cell/progenitor cell markers in MSCs. (a) The stem cell marker BMI1 (green) expression is observed in all MSCs. Nuclei are counterstained with Hoechst (blue). Scale Bar: 100 μ m. (b–d) Relative mRNA expression of stem cell/progenitor markers *ABCG2* (b), *NANOG* (c), and *SOX2* (d) in MSCs was measured by RT-PCR. Gene expression was normalized to CSSC (red bars). $N = 2$ cell lines for BMMSCs and UCSCs. Results are expressed as mean \pm SEM. Statistical analysis: ANOVA comparison of the means, followed by Tukey’s test. * $P < 0.05$.

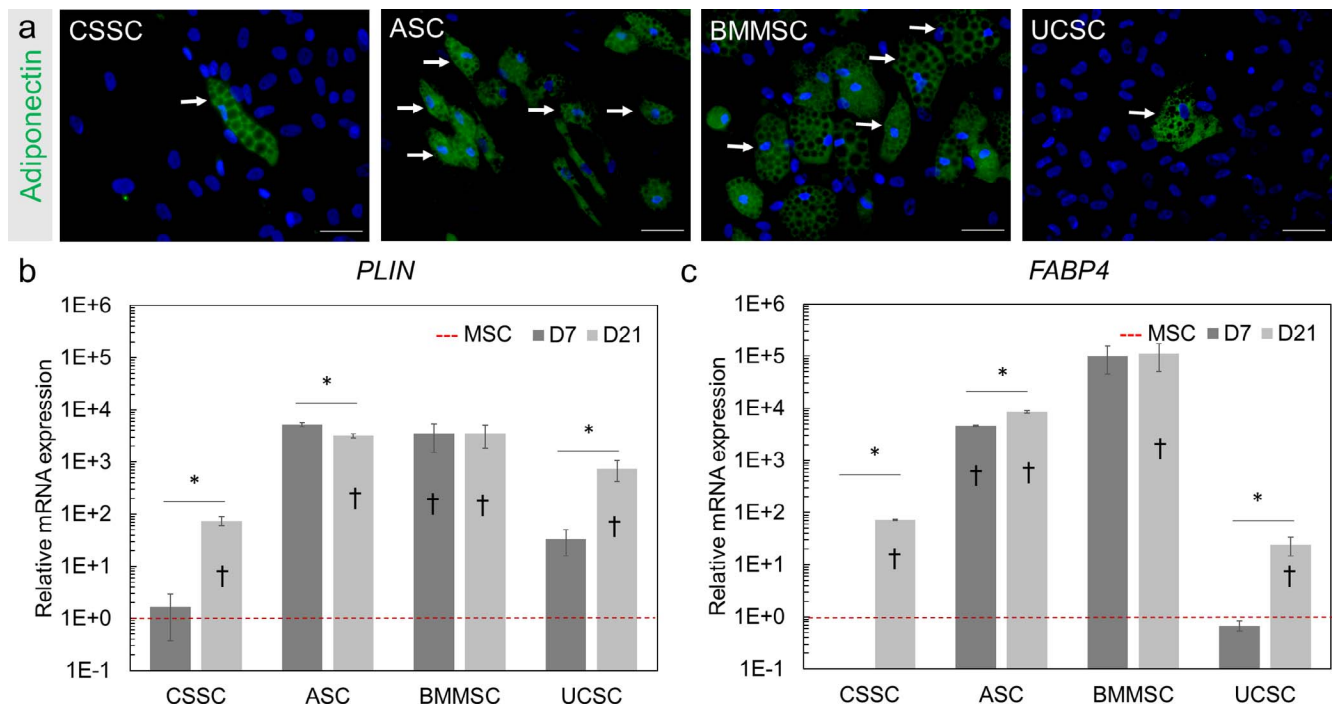


FIGURE 3. Adipogenic differentiation potential of the MSCs. (a) Lipid aggregations were visualized by immunofluorescence staining of adiponectin (green) in MSCs after 21 days of differentiation. Hoechst was used as nuclear counterstaining (blue). White arrows indicate examples of the observed lipid vacuoles. Scale Bar: 50 μ m. (b, c) Gene expression analysis of the adipose-related markers *PLIN* (b) and *FABP4* (c) was performed by RT-PCR for the MSCs at day 7 (D7) and day 21 (D21) of adipogenic differentiation. Gene expression was normalized to the undifferentiated parental cells (MSC, red dotted line set at 1). Results are expressed as mean \pm SEM. $N = 2$ cell lines for BMMSC and UCSC. Statistical analysis: ANOVA followed by Tukey’s test comparison of means. * $P < 0.05$; † $P < 0.05$ comparison to the respective undifferentiated MSCs.

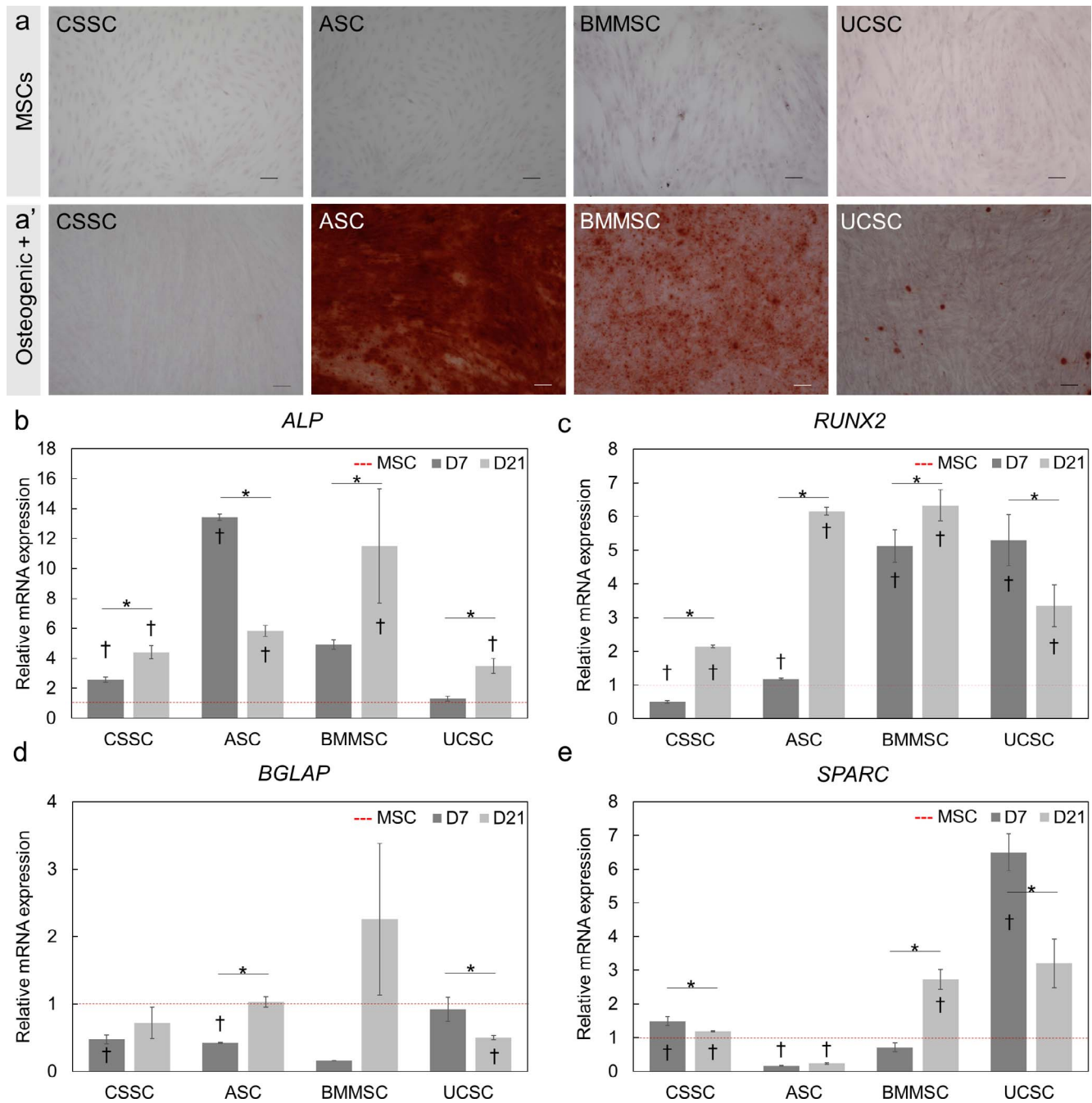


FIGURE 4. Osteogenic differentiation potential of the human MSCs. (a, a') Alizarin red staining of undifferentiated MSCs (a) and 21-day differentiated MSCs (a') was used to visualize calcium depositions. Alizarin red staining was strongly observed in ASCs and BMMSCs at day 21. *Scale Bar:* 100 μ m. (b–e) Transcript analysis of osteogenic markers: ALP (b), RUNX2 (c), BGLAP (d), and SPARC (e) after 7 (D7) and 21 (D21) days of induction. *Red dotted line* is the undifferentiated parental cells (MSC) normalized to 1. Results are expressed as mean \pm SEM. $N = 2$ cell lines for BMMSCs and UCSCs. Statistical analysis: ANOVA followed by Tukey's test comparison of means. * $P < 0.05$; † $P < 0.05$ comparison to the respective undifferentiated MSCs.

comparison). CSSCs showed 30-fold higher expression of *SOX2* ($P < 0.05$) than did the other MSCs. These findings suggest that the MSCs under investigation are proliferating and expressing stem/progenitor markers and the appropriate MSC markers.

Multilineage Differentiation

MSCs have the potential to differentiate into a variety of cell lineages in vitro.⁴⁰ Therefore, we investigated the MSCs for their differentiation potential toward adipocytes, osteoblasts,

and chondrocytes. The differentiation was confirmed with immunohistochemistry and expression of lineage-specific transcripts before and after induction of differentiation.

After adipogenic differentiation for 21 days, fat droplets were observed with bright-field microscopy among cultures of CSSCs, ASCs, and BMMSCs. We confirmed these observations by immunofluorescence staining of adiponectin, an adipocyte-specific protein,⁴⁴ after 21 days of differentiation in all MSCs (white arrows, Fig. 3a) as well as gene expression analysis of perilipin (*PLIN*) and fatty acid binding protein 4 (*FABP4*)

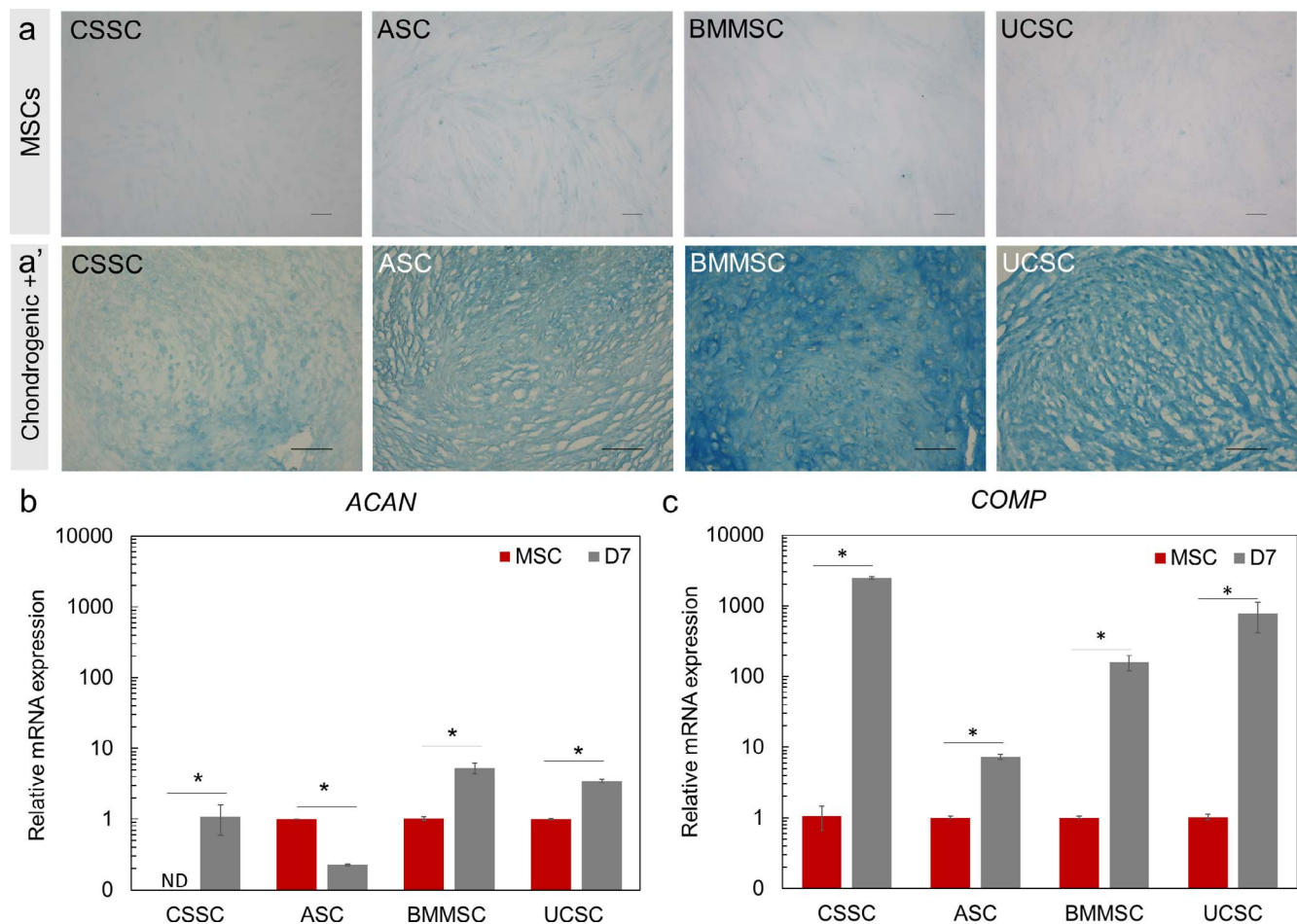


FIGURE 5. Chondrogenic differentiation potential of the MSCs investigated. (a, a') Undifferentiated MSCs (a) and cryosections from 21-day differentiated MSC pellets (a') were stained with Alcian blue to visualize chondrocyte-associated extracellular proteoglycans. Alcian blue staining was detected in all MSCs, especially BMMSCs. Scale Bar: 100 μ m. (b, c) Transcript analysis of chondrogenic markers ACAN (b) and COMP (c) was performed by RT-PCR after 7 days (gray bars) of induction and the expression was normalized to the undifferentiated parental cells (MSC, red bars). Because there was no detection in ACAN transcripts in the CSSC undifferentiated sample (MSC), the data were normalized at 1 for the chondrogenic-induced sample (D7 induction). Results are expressed as mean \pm SEM. $N = 2$ cell lines for BM MSCs and UC SCs. Statistical analysis: ANOVA followed by Student *t*-test comparison of means. * $P < 0.05$. ND, not detected.

transcripts as differentiation markers.⁴⁵ After 7 and 21 days of differentiation toward the adipogenic lineage, the expression level of *FABP4* increased by more than 24-fold ($P < 0.05$) and the expression of *PLIN* increased by 74-fold ($P < 0.05$) in all MSCs (Figs. 3b, 3c). The greatest increase in expression of both markers and the greatest adiponectin staining were detected in BMMSCs and ASCs; this finding demonstrates a greater differentiation potential toward an adipogenic lineage after 21 days of differentiation.

Osteogenic differentiation was evaluated by detecting calcium depositions with Alizarin red staining after 21 days of differentiation (Fig. 4a). Staining of MSCs with Alizarin red solution did not indicate any calcium depositions before differentiation (Fig. 4a). Strong Alizarin red staining was observed in the differentiated ASCs and, to a lesser extent, in BMMSCs, UCSCs, and CSSCs after 21 days of differentiation (Fig. 4a). To confirm these observations, the expression of four osteoblast-associated genes was analyzed at days 7 and 21 of differentiation: alkaline phosphatase (*ALP*), runt-related transcription factor 2 (*RUNX2*),⁴⁶ osteocalcin (*BGLAP*),⁴⁷ and osteonectin (*SPARC*).⁴⁸ *ALP* expression was upregulated by 3.5-fold ($P < 0.05$) in all differentiated MSCs (Fig. 4b). *RUNX2* mRNA levels were elevated ($P < 0.05$) more than 2.1-fold after 7 and 21 days of differentiation of all MSCs (Fig. 4c). *BGLAP* expression was not

increased in any of the MSC types after differentiation for 7 or 21 days (Fig. 4d). *SPARC* expression was upregulated 6.5-fold in UCSCs and 1.5-fold in CSSCs ($P < 0.05$) on day 7, and *SPARC* expression was upregulated 2.7-fold in BMMSCs on day 21 of differentiation (Fig. 4e). *SPARC* expression was downregulated in ASCs after 7 and 21 days of differentiation. These results can be explained by the later expression of *SPARC* and *BGLAP* during osteogenic differentiation.^{47–49} Twenty-one days of differentiation was not long enough to stimulate the increased expression of those genes in the investigated MSCs; this finding has been observed previously in another study of BMMSCs.⁴⁶ Overall, ASCs and BMMSCs displayed the most Alizarin red staining, and this staining was correlated with increased levels of *ALP* and *RUNX2* after differentiation.

Chondrogenic differentiation was observed in sections of 21-day pellets by Alcian blue staining, which detected chondrocyte-associated extracellular proteoglycans (Fig. 5a'). Undifferentiated MSCs did not express chondrocyte-specific proteoglycans (Fig. 5a). Aggrecan (*ACAN*) and cartilage oligomeric matrix protein (*COMP*) were used to confirm chondrogenic differentiation after 7 days of differentiation.^{50,51} *ACAN* had a higher expression level in BMMSCs (5.4-fold higher, $P < 0.05$) and UCSCs (3.7-fold higher, $P < 0.05$) after differentiation (Fig. 5b). Decreased expression of *ACAN* was

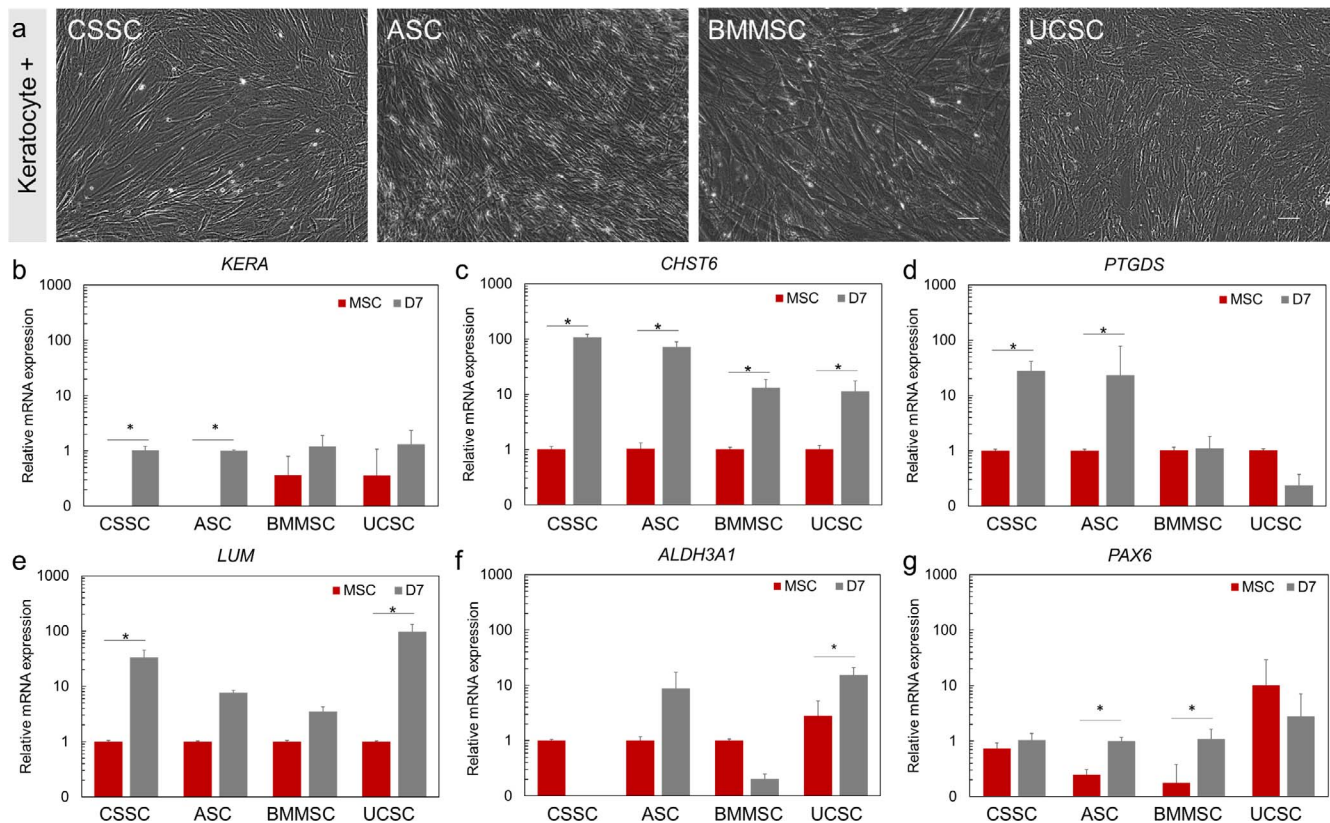


FIGURE 6. Keratocyte lineage induction of the MSCs. (a) Phase-contrast microscopy pictures of the MSCs after 7 days of keratocyte induction. *Scale Bar:* 100 μ m for CSSC, ASC, and UC SC, 50 μ m for BM MSC. (b–g) Expression of the keratocyte and markers: KERA (b), CHST6 (c), PTGDS (d), LUM (e), ALDH3A1 (f), and PAX6 (g) after 7 days of keratocyte differentiation. The expression was normalized to the undifferentiated parental cells (MSCs, set at 1, red bars). Results are expressed as mean \pm SEM. $N = 2$ cell lines for BMMSC and UCSC. Statistical analysis: ANOVA followed by Student's *t*-test comparison of means. * $P < 0.05$.

observed in ASCs after 7 days of differentiation. Undifferentiated CSSCs did not express *ACAN* (not detected, Fig. 5b); therefore, the expression level of *ACAN* in differentiated CSSCs was arbitrarily normalized to 1 (Fig. 5b). *COMP* had a minimal increase in expression (7.2-fold increase; $P < 0.05$) in all MSC types at 7 days of chondrogenic differentiation (Fig. 5c). In summary, strong Alcian blue staining was observed in BMMSCs and UCSCs that also showed high levels of *ACAN* and *COMP* expression; thus, BMMSCs and UCSCs demonstrated a higher degree of differentiation toward the chondrogenic lineage than did ASCs and CSSCs after 21 days.

Differentiation into Keratocyte Lineage

After 7 days of keratocyte induction, MSCs demonstrated morphologic changes that involved long cell processes that are characteristic of quiescent keratocytes (Fig. 6a). Keratocytes are highly enriched in specific proteoglycans, such as keratocan and lumican,^{52,53} corneal crystallins, such as aldehyde dehydrogenase 3A1,⁵⁴ and the eicosanoid metabolic enzyme PGD2 synthase.⁵⁵ Keratocytes also express a large amount of *CHST6*, which encodes a carbohydrate sulfotransferase involved in keratan sulfate biosynthesis.⁵⁶

After 7 days of differentiation, the expression of the keratocyte markers *KERA*, *CHST6*, *LUM*, and *PTGDS* was upregulated at least 24-fold in differentiated CSSCs ($P < 0.05$) (Figs. 6b–e). After differentiation, ASCs showed at least a 23-fold increase ($P < 0.05$) in expression of *KERA*, *CHST6*, and *PTGDS* markers (Figs. 6b–d; Supplementary Fig. S1). A 13-fold increase in expression of *CHST6* was observed in differentiated

BMMSCs ($P < 0.05$, Fig. 6c). The expression of *CHST6* and *LUM* was upregulated at least 11-fold in differentiated UCSCs ($P < 0.05$, Figs. 6c, 6e). A 15-fold upregulation of *ALDH3A1* expression was detected in differentiated UCSCs only ($P < 0.05$, Fig. 6f). The expression of *PAX6*, which serves an important role in ocular development³¹ and for corneal keratocyte progenitors,⁵⁷ was also investigated. ASCs and BMMSCs showed a 4.5-fold increase in expression of *PAX6* after keratocyte differentiation (Fig. 6g).

In summary, CSSCs and ASCs demonstrated the highest level of differentiation capacity toward keratocyte lineage after 7 days of differentiation, as indicated by the increased expression of the markers we investigated.

Anti-inflammatory Response of MSCs

We analyzed the expression of *TNFAIP6* by the MSCs after stimulation with the proinflammatory cytokines IFN- γ and TNF- α . *TNFAIP6* encodes the TSG-6 protein, which through its anti-inflammatory properties promotes corneal wound healing with reduced scar formation.⁸ We observed a 3-fold increase ($P < 0.05$) in the production of *TNFAIP6* by stimulated CSSCs, whereas ASCs, BMMSCs, and UCSCs did not show any significant increase in *TNFAIP6* production after stimulation (Fig. 7; Supplementary Fig. S2).

DISCUSSION

The therapeutic potential of MSCs has been explored in corneal stromal wound healing.^{20–22} ASCs, UCSCs, and

BMMSCs have been shown to improve corneal opacity *in vivo* with differentiation of the MSCs into keratocytes after they have been applied to the injured or scarred cornea.^{20–22} Studies have shown that human MSCs derived from different tissues can differentiate toward the keratocyte lineage *in vitro*, and these MSC types include ASCs,^{52,58–60} BMMSCs,²¹ periodontal ligament stem cells,^{27,29} dental pulp stem cells,²⁶ UCSCs,²⁸ turbinate-derived MSCs,²³ and CSSCs.^{8,25,61} However, there is no direct comparative study of keratocyte differentiation of MSCs derived from different tissue types. Therefore, we investigated the potential of four different types of MSCs (i.e., ASCs, BMMSCs, UCSCs, and CSSCs) to differentiate into the corneal keratocyte lineage.

Characterization of the four sources of MSCs used in our study shows that they are adult stem cells as defined by the ISCT,⁴⁰ but only 75% of the CSSCs were CD90+. Other studies have shown the stable expression of CD90, which meets the ISCT criterion of more than 95% of positive cells^{62–64}; in one study, approximately 90% of cells ($89.87\% \pm 8.8\%$) expressed CD90.⁶⁵ Possible explanations for this discrepancy of CD90 expression are the heterogeneity of the cell population at the time of analysis and the use of a CSSC culture medium that was different from the media used for the other types of MSCs. The role of CD90 in MSCs is currently unknown; therefore, we are unaware of the consequences that the lower expression of CD90 would have on CSSCs. The multilineage differentiation of MSCs toward adipocytes, osteocytes, and chondrocytes was achieved among all types of MSCs that we investigated. Adipogenic differentiation was observed to be the greatest among BMMSCs and ASCs. Consistent with our results, Han and colleagues⁶⁶ demonstrated that UCSCs had lower adipogenic differentiation capacity than do BMMSCs and ASCs. We also demonstrated that all four types of MSCs were able to differentiate into chondrocytes and the greatest potential for this differentiation was attributed to BMMSCs.

Our results indicated that ASCs had high plasticity for the osteogenic lineage with a strong Alizarin red staining. In previous studies, osteogenic differentiation was lower in ASCs compared with BMMSCs.^{67,68} In CSSCs, the lack of Alizarin red staining and lower increase in *ALP* and *RUNX2* expression suggested that the degree of osteogenic differentiation was the lowest in CSSCs than in the other types of MSCs. Our results suggest that the differentiation of MSCs occurs with lineage-specific capacities as a varying degree of differentiation was observed for each MSC type at the time points investigated in this study.

Lee and colleagues¹⁹ first demonstrated that the potential of human MSCs for osteogenic differentiation correlated negatively with the efficacy of the human MSCs to decrease corneal inflammation *in vivo*. In addition to this observation, the authors showed that the efficacy of the MSCs was attributed to the production of TSG-6 protein. Similarly, a negative correlation between osteogenic differentiation potential and *TNFAIP6* levels was observed.¹⁹ TSG-6, which is produced by MSCs, is directly involved in the reduction of corneal inflammation by decreasing neutrophil migration to the wound site; this reduced migration promotes wound healing without scar formation.^{8,69} Our results indicated that of all types of MSCs tested, only CSSCs were induced to express *TNFAIP6* (3-fold increase compared with the control), paralleling its lessened osteogenic differentiation capacity.

During corneal repair, keratocytes play a key role in the wound-healing process that by default leads to corneal fibrosis and corneal opacity.^{36,70} The differentiation into a keratocyte phenotype has been demonstrated in ASCs,^{52,59,60} BMMSCs,²⁴ and bioengineered cornea with Wharton's jelly-derived MSCs.²⁸ The current study again confirms that MSCs can

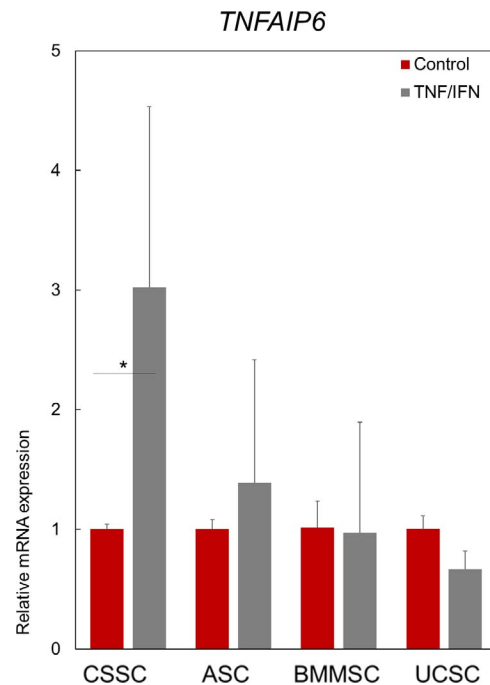


FIGURE 7. The response of MSCs to proinflammatory cytokines. Anti-inflammatory response of the MSCs to by proinflammatory cytokines IFN- γ and TNF- α as quantified by *TNFAIP6* transcript analysis. Data are normalized to the respective unstimulated cells (control, red bars set at 1). Results are expressed as mean \pm SEM. $N = 2$ cell lines for BMMSC and UCSC. Statistical analysis: ANOVA followed by Student's *t*-test comparison of means. * $P < 0.05$.

differentiate into cells of the keratocyte lineage. Among the four types of MSCs investigated, CSSCs and ASCs appear to have the greatest potential to differentiate into cells of the keratocyte lineage. CSSCs derive from a neural crest origin,⁷¹ as do some of the cells in the ASC population.⁷² Dental pulp stem cells, which also have neural crest origin, were also observed to differentiate into keratocyte-like cells.²⁶ These results suggest that embryonic lineage may have some influence in the keratocyte differentiation potential of stem cells. The potential of the cells to differentiate into cells of the corneal stromal lineage might be important for selection of suitable sources of MSCs for corneal wound-healing therapy (e.g., CSSCs and ASCs).

Studies have shown that CSSC application to a mouse model of corneal wounding stimulates regeneration of corneal transparency without scar formation.^{7,8,37,73} Preliminary clinical results have appeared to be promising, as patients treated with autologous and allogeneic CSSCs have recovered some visual acuity (Funderburgh JL, et al. *IOVS* 2018;58:ARVO E-Abstract 3371). In view of that, MSC-based therapies may permit the use of autologous treatment, thereby eliminating the need for donor tissue and corneal transplantation. In addition, autologous use of MSCs lowers the risk of graft-versus-host disease.⁷⁴

Cell culture models allowed us to explore the potential of MSCs to differentiate into keratocytes, produce corneal extracellular components, and exert anti-inflammatory properties. For purposes of autologous treatment, we need to consider the accessibility of MSCs from patients. ASCs, being easily accessible,⁶⁶ may serve as a suitable MSC source to generate effective and robust cell therapy. CSSCs are a great candidate as well, given their putative anti-inflammatory properties. Although CSSC isolation could be considered more invasive, they were identified in limbal biopsies for

ocular surface reconstruction,⁷⁵ and can be propagated in vitro.³⁷ Limbal biopsies are well-established and heal with few complications.⁷⁶ UCSC isolation is circumstantially challenging. Banking UCSCs is currently more common,⁷⁷ but the source is still scarce. To identify the most effective, practical, and accessible MSC types, we need to evaluate the potential of each of the four investigated MSC types to reduce scar formation and inflammation in the living eye. Therefore, further investigation of these types of MSCs in in vivo corneal wound models would offer essential information about the potential of MSCs to repair corneal tissue.

Acknowledgments

Supported by a department unrestricted fund from Research to Prevent Blindness (SXD), National Institutes of Health EY016415 (JLF), Eye and Ear Foundation of Pittsburgh, Stein Innovator Award from Research to Prevent Blindness (JLF), and Department of Defense W81WH-14-1-0465 (JLF).

Disclosure: **A. Dos Santos**, None; **A. Balayan**, None; **M.L. Funderburgh**, None; **J. Ngo**, None; **J.L. Funderburgh**, None; **S.X. Deng**, None

References

- Pascolini D, Mariotti SP. Global estimates of visual impairment: 2010. *Br J Ophthalmol*. 2012;96:614–618.
- Whitcher JP, Srinivasan M, Upadhyay MP. Corneal blindness: a global perspective. *Bull World Health Organ*. 2001;79:214–221.
- Tan DT, Dart JK, Holland EJ, Kinoshita S. Corneal transplantation. *Lancet*. 2012;379:1749–1761.
- Gain P, Jullienne R, He Z, et al. Global survey of corneal transplantation and eye banking. *JAMA Ophthalmol*. 2016;134:167–173.
- Griffith M, Jackson WB, Lagali N, Merrett K, Li F, Fagerholm P. Artificial corneas: a regenerative medicine approach. *Eye (Lond)*. 2009;23:1985–1989.
- Liu W, Merrett K, Griffith M, et al. Recombinant human collagen for tissue engineered corneal substitutes. *Biomaterials*. 2008;29:1147–1158.
- Du Y, Carlson EC, Funderburgh ML, et al. Stem cell therapy restores transparency to defective murine corneas. *Stem Cells*. 2009;27:1635–1642.
- Hertsenberg AJ, Shojaati G, Funderburgh ML, Mann MM, Du Y, Funderburgh JL. Corneal stromal stem cells reduce corneal scarring by mediating neutrophil infiltration after wounding. *PLoS One*. 2017;12:e0171712.
- Arnalich-Montiel F, Pastor S, Blazquez-Martinez A, et al. Adipose-derived stem cells are a source for cell therapy of the corneal stroma. *Stem Cells*. 2008;26:570–579.
- Li F, Zhao SZ. Mesenchymal stem cells: potential role in corneal wound repair and transplantation. *World J Stem Cells*. 2014;6:296–304.
- Bianco P, Riminucci M, Gronthos S, Robey PG. Bone marrow stromal stem cells: nature, biology, and potential applications. *Stem Cells*. 2001;19:180–192.
- Zuk PA, Zhu M, Ashjian P, et al. Human adipose tissue is a source of multipotent stem cells. *Mol Biol Cell*. 2002;13:4279–4295.
- Mennan C, Wright K, Bhattacharjee A, Balain B, Richardson J, Roberts S. Isolation and characterisation of mesenchymal stem cells from different regions of the human umbilical cord. *Biomed Res Int*. 2013;2013:916136.
- Pierdomenico L, Bonsi L, Calvitti M, et al. Multipotent mesenchymal stem cells with immunosuppressive activity can be easily isolated from dental pulp. *Transplantation*. 2005;80:836–842.
- Funderburgh JL, Funderburgh ML, Du Y. Stem cells in the limbal stroma. *Ocul Surf*. 2016;14:113–120.
- Ullah I, Subbarao RB, Rho GJ. Human mesenchymal stem cells—current trends and future prospective. *Biosci Rep*. 2015;35:e00191.
- Lan Y, Kodati S, Lee HS, Omoto M, Jin Y, Chauhan SK. Kinetics and function of mesenchymal stem cells in corneal injury. *Invest Ophthalmol Vis Sci*. 2012;53:3638–3644.
- Oh JY, Lee RH, Yu JM, et al. Intravenous mesenchymal stem cells prevented rejection of allogeneic corneal transplants by aborting the early inflammatory response. *Mol Ther*. 2012;20:2143–2152.
- Lee RH, Yu JM, Fokkett AM, et al. TSG-6 as a biomarker to predict efficacy of human mesenchymal stem/progenitor cells (hMSCs) in modulating sterile inflammation in vivo. *Proc Natl Acad Sci U S A*. 2014;111:16766–16771.
- Demirayak B, Yuksel N, Celik OS, et al. Effect of bone marrow and adipose tissue-derived mesenchymal stem cells on the natural course of corneal scarring after penetrating injury. *Exp Eye Res*. 2016;151:227–235.
- Liu H, Zhang J, Liu CY, Hayashi Y, Kao WW. Bone marrow mesenchymal stem cells can differentiate and assume corneal keratocyte phenotype. *J Cell Mol Med*. 2012;16:1114–1124.
- Liu H, Zhang J, Liu CY, et al. Cell therapy of congenital corneal diseases with umbilical mesenchymal stem cells: lumican null mice. *PLoS One*. 2010;5:e10707.
- Park M, Kim B, Kim H, et al. Human turbinate-derived mesenchymal stem cells differentiated into keratocyte progenitor cells. *J Clin Exp Ophthalmol*. 2017;8:8.
- Park SH, Kim KW, Chun YS, Kim JC. Human mesenchymal stem cells differentiate into keratocyte-like cells in keratocyte-conditioned medium. *Exp Eye Res*. 2012;101:16–26.
- Du Y, Sundarraj N, Funderburgh ML, Harvey SA, Birk DE, Funderburgh JL. Secretion and organization of a cornea-like tissue in vitro by stem cells from human corneal stroma. *Invest Ophthalmol Vis Sci*. 2007;48:5038–5045.
- Syed-Picard FN, Du Y, Lathrop KL, Mann MM, Funderburgh ML, Funderburgh JL. Dental pulp stem cells: a new cellular resource for corneal stromal regeneration. *Stem Cells Transl Med*. 2015;4:276–285.
- Chen J, Zhang W, Backman IJ, Kelk P, Danielson P. Mechanical stress potentiates the differentiation of periodontal ligament stem cells into keratocytes. *Br J Ophthalmol*. 2018;102:562–569.
- Garzon I, Martin-Piedra MA, Alfonso-Rodriguez C, et al. Generation of a biomimetic human artificial cornea model using Wharton's jelly mesenchymal stem cells. *Invest Ophthalmol Vis Sci*. 2014;55:4073–4083.
- Yam GH, Teo EP, Setiawan M, et al. Postnatal periodontal ligament as a novel adult stem cell source for regenerative corneal cell therapy. *J Cell Mol Med*. 2018;22:3119–3132.
- Hay ED, Linsenmayer TF, Trelstad RL, von der Mark K. Origin and distribution of collagens in the developing avian cornea. *Curr Top Eye Res*. 1979;1:1–35.
- West-Mays JA, Dwivedi DJ. The keratocyte: corneal stromal cell with variable repair phenotypes. *Int J Biochem Cell Biol*. 2006;38:1625–1631.
- Sloniecka M, Le Roux S, Boman P, Bystrom B, Zhou Q, Danielson P. Expression profiles of neuropeptides, neurotransmitters, and their receptors in human keratocytes in vitro and in situ. *PLoS One*. 2015;10:e0134157.
- Jester JV, Moller-Pedersen T, Huang J, et al. The cellular basis of corneal transparency: evidence for 'corneal crystallins'. *J Cell Sci*. 1999;112:613–622.

34. Zieske JD. Corneal development associated with eyelid opening. *Int J Dev Biol.* 2004;48:903-911.
35. Girard MT, Matsubara M, Kublin C, Tessier MJ, Cintron C, Fini ME. Stromal fibroblasts synthesize collagenase and stromelysin during long-term tissue remodeling. *J Cell Sci.* 1993;104:1001-1011.
36. Fini ME. Keratocyte and fibroblast phenotypes in the repairing cornea. *Prog Retin Eye Res.* 1999;18:529-551.
37. Basu S, Hertszenberg AJ, Funderburgh ML, et al. Human limbal biopsy-derived stromal stem cells prevent corneal scarring. *Sci Transl Med.* 2014;6:266ra172.
38. Reinisch A, Strunk D. Isolation and animal serum free expansion of human umbilical cord derived mesenchymal stromal cells (MSCs) and endothelial colony forming progenitor cells (ECFCs). *J Vis Exp.* 2009;2009:1525.
39. Livak KJ, Schmittgen TD. Analysis of relative gene expression data using real-time quantitative PCR and the 2(-Delta Delta C(T)) Method. *Methods.* 2001;25:402-408.
40. Dominici M, Le Blanc K, Mueller I, et al. Minimal criteria for defining multipotent mesenchymal stromal cells. The International Society for Cellular Therapy position statement. *Cytotherapy.* 2006;8:315-317.
41. Lee JY, Yu KR, Kim HS, et al. BMI1 inhibits senescence and enhances the immunomodulatory properties of human mesenchymal stem cells via the direct suppression of MKP-1/DUSP1. *Aging (Albany NY).* 2016;8:1670-1689.
42. Du Y, Funderburgh ML, Mann MM, SundarRaj N, Funderburgh JL. Multipotent stem cells in human corneal stroma. *Stem Cells.* 2005;23:1266-1275.
43. Zhang S, Cui W. Sox2, a key factor in the regulation of pluripotency and neural differentiation. *World J Stem Cells.* 2014;6:305-311.
44. Lihn AS, Pedersen SB, Richelsen B. Adiponectin: action, regulation and association to insulin sensitivity. *Obes Rev.* 2005;6:13-21.
45. Shan T, Liu W, Kuang S. Fatty acid binding protein 4 expression marks a population of adipocyte progenitors in white and brown adipose tissues. *FASEB J.* 2013;27:277-287.
46. Wang L, Li ZY, Wang YP, Wu ZH, Yu B. Dynamic expression profiles of marker genes in osteogenic differentiation of human bone marrow-derived mesenchymal stem cells. *Chin Med Sci J.* 2015;30:108-113.
47. Tsao YT, Huang YJ, Wu HH, Liu YA, Liu YS, Lee OK. Osteocalcin mediates biomineralization during osteogenic maturation in human mesenchymal stromal cells. *Int J Mol Sci.* 2017;18:159.
48. Nuttelman CR, Tripodi MC, Anseth KS. In vitro osteogenic differentiation of human mesenchymal stem cells photo-encapsulated in PEG hydrogels. *J Biomed Mater Res A.* 2004;68:773-782.
49. Rutkovskiy A, Stenslokken KO, Vaage IJ. Osteoblast differentiation at a glance. *Med Sci Monit Basic Res.* 2016;22:95-106.
50. Solchaga LA, Penick KJ, Welter JF. Chondrogenic differentiation of bone marrow-derived mesenchymal stem cells: tips and tricks. *Methods Mol Biol.* 2011;698:253-278.
51. Xu J, Wang W, Ludeman M, et al. Chondrogenic differentiation of human mesenchymal stem cells in three-dimensional alginate gels. *Tissue Eng Part A.* 2008;14:667-680.
52. Du Y, Roh DS, Funderburgh ML, et al. Adipose-derived stem cells differentiate to keratocytes in vitro. *Mol Vis.* 2010;16:2680-2689.
53. Funderburgh JL, Mann MM, Funderburgh ML. Keratocyte phenotype mediates proteoglycan structure: a role for fibroblasts in corneal fibrosis. *J Biol Chem.* 2003;278:45629-45637.
54. Estey T, Piatigorsky J, Lassen N, Vasiliou V. ALDH3A1: a corneal crystallin with diverse functions. *Exp Eye Res.* 2007;84:3-12.
55. Chakravarti S, Wu F, Vij N, Roberts L, Joyce S. Microarray studies reveal macrophage-like function of stromal keratocytes in the cornea. *Invest Ophthalmol Vis Sci.* 2004;45:3475-3484.
56. Di Iorio E, Barbaro V, Volpi N, et al. Localization and expression of CHST6 and keratan sulfate proteoglycans in the human cornea. *Exp Eye Res.* 2010;91:293-299.
57. Funderburgh ML, Du Y, Mann MM, SundarRaj N, Funderburgh JL. PAX6 expression identifies progenitor cells for corneal keratocytes. *FASEB J.* 2005;19:1371-1373.
58. Ahearne M, Lysaght J, Lynch AP. Combined influence of basal media and fibroblast growth factor on the expansion and differentiation capabilities of adipose-derived stem cells. *Cell Regen (Lond).* 2014;3:13.
59. Zhang S, Espandar L, Imhof KM, Bunnell BA. Differentiation of human adipose-derived stem cells along the keratocyte lineage in vitro. *J Clin Exp Ophthalmol.* 2013;4:11435.
60. Lynch AP, Ahearne M. Retinoic acid enhances the differentiation of adipose-derived stem cells to keratocytes in vitro. *Trans Vis Sci Tech.* 2017;6(1):6.
61. Byun YS, Tibrewal S, Kim E, et al. Keratocytes derived from spheroid culture of corneal stromal cells resemble tissue resident keratocytes. *PLoS One.* 2014;9:e112781.
62. Branch MJ, Hashmani K, Dhillon P, Jones DR, Dua HS, Hopkinson A. Mesenchymal stem cells in the human corneal limbal stroma. *Invest Ophthalmol Vis Sci.* 2012;53:5109-5116.
63. Hashmani K, Branch MJ, Sidney LE, et al. Characterization of corneal stromal stem cells with the potential for epithelial transdifferentiation. *Stem Cell Res Ther.* 2013;4:75.
64. Matthyssen S, Ni Dhubhghaill S, Van Gerwen V, Zakaria N. Xeno-free cultivation of mesenchymal stem cells from the corneal stroma. *Invest Ophthalmol Vis Sci.* 2017;58:2659-2665.
65. Vereb Z, Poliska S, Albert R, et al. Role of human corneal stroma-derived mesenchymal-like stem cells in corneal immunity and wound healing. *Sci Rep.* 2016;6:26227.
66. Han I, Kwon BS, Park HK, Kim KS. Differentiation potential of mesenchymal stem cells is related to their intrinsic mechanical properties. *Int Neurolog J.* 2017;21:S24-31.
67. Xu L, Liu Y, Sun Y, et al. Tissue source determines the differentiation potentials of mesenchymal stem cells: a comparative study of human mesenchymal stem cells from bone marrow and adipose tissue. *Stem Cell Res Ther.* 2017;8:275.
68. Zhang L, Coulson-Thomas VJ, Ferreira TG, Kao WW. Mesenchymal stem cells for treating ocular surface diseases. *BMC Ophthalmol.* 2015;15(suppl 1):155.
69. Oh JY, Roddy GW, Choi H, et al. Anti-inflammatory protein TSG-6 reduces inflammatory damage to the cornea following chemical and mechanical injury. *Proc Natl Acad Sci U S A.* 2010;107:16875-16880.
70. Torricelli AA, Santhanam A, Wu J, Singh V, Wilson SE. The corneal fibrosis response to epithelial-stromal injury. *Exp Eye Res.* 2016;142:110-118.
71. Yoshida S, Shimmura S, Nagoshi N, et al. Isolation of multipotent neural crest-derived stem cells from the adult mouse cornea. *Stem Cells.* 2006;24:2714-2722.
72. Sowa Y, Imura T, Numajiri T, et al. Adipose stromal cells contain phenotypically distinct adipogenic progenitors derived from neural crest. *PLoS One.* 2013;8:e84206.
73. Shojaati G, Khandaker I, Sylakowski K, Funderburgh ML, Du Y, Funderburgh JL. Compressed collagen enhances stem cell therapy for corneal scarring. *Stem Cells Transl Med.* 2018;7:487-494.

74. Thompson RW Jr, Price MO, Bowers PJ, Price FW Jr. Long-term graft survival after penetrating keratoplasty. *Ophthalmology*. 2003;110:1396-1402.
75. Polisetty N, Fatima A, Madhira SL, Sangwan VS, Vemuganti GK. Mesenchymal cells from limbal stroma of human eye. *Mol Vis*. 2008;14:431-442.
76. Basu S, Sureka SP, Shanbhag SS, Kethiri AR, Singh V, Sangwan VS. Simple limbal epithelial transplantation: long-term clinical outcomes in 125 cases of unilateral chronic ocular surface burns. *Ophthalmology*. 2016;123:1000-1010.
77. Butler MG, Menitove JE. Umbilical cord blood banking: an update. *J Assist Reprod Genet*. 2011;28:669-676.